Available online at www.sciencedirect.com

ScienceDirect

Procedia Engineering 109 (2015) 473 – 483

Procedia Engineering

www.elsevier.com/locate/procedia

XXIII Italian Group of Fracture Meeting, IGFXXIII

Crack growth behavior of welded stiffened panel

Raffaele Sepe[a]*, Enrico Armentani[a], Pasquale di Lascio[b], Roberto Citarella[b]

[a]*Department. of Chemical, Materials and Production Engineering - University of Naples Federico II - P.le V. Tecchio, 80 - 80125 Naples, Italy*
[b]*Department of Industrial Engineering, University of Salerno Fisciano (SA), Italy*

Abstract

Fatigue crack growth experimental tests and numerical analyses on Friction Stir Welding (FSW) welded flat stiffened panels were performed in order to assess their fracture resistance capability. Panels and stiffeners are made of aluminum alloy 2024-T3. Linear elastic FEM (Finite Element Method) and DBEM (Dual Boundary Element Method) stress analyses were performed to simulate crack growth, obtaining a satisfactory correlation against experimental outcomes.

Peer-review under responsibility of the Gruppo Italiano Frattura (IGF)

Keywords: cracks; FEM; DBEM; non-linear analysis; stiffned panel

1. Introduction

Design, analysis and verification of damage tolerant structures involve both structural characterization and damage detection assessment. Methods to determine fatigue performance, crack growth and residual strength of complex details have improved significantly since the introduction of commercial jet transports. Therefore, new tailored and cost-effective materials are continuously designed and tested to realize high-performance aircraft structures. Nowadays, the tendency in aircraft industry is aimed at obtaining integral structures in composite materials or metals by manufacturing processes such as welding and bonding rather than the traditional riveting joining methods.

Significant improvement have been made in the prediction capability of fatigue crack propagation and many design techniques have been developed using either more complex analytical formulations or numerical methods [1-5]. To support these theoretical analyses it is necessary to carry out experimental investigations that should take in account the actual specimen shape, size and boundary conditions. As a matter of fact a key step of the airframe design and

* Corresponding author. Tel.: +39-081-768-24-50; fax: +39-081-768-21-72.
E-mail address: raffsepe@unina.it

Peer-review under responsibility of the Gruppo Italiano Frattura (IGF)
doi:10.1016/j.proeng.2015.06.251

certification process is the full-scale fatigue test, where a complete airframe structure is subjected to realistic spectrum loads, representative of those predicted to occur over the life-of-type. Generally, these fatigue tests are cycled until the equivalent of several lifetimes is achieved or a failure occurs.

Several full-scale experimental investigations have been carried out to predict the fatigue life of aerospace components [6-9]. Armentani et al. [10] carried out experimental and numerical investigations on the application of innovative materials, obtained by the use of improved lamina and fibre reinforcements (FML) to panels of a typical wide body fuselage section. The tested panel was full scale and underwent a bi-axial fatigue load, applied by means of a multiaxial fatigue machine [11].

The focus of the paper is on crack growth tests and numerical analyses on Friction Stir Welding (FSW) welded flat stiffened panels. All fatigue tests were performed by a dedicated test machine on flat stiffened panels. Afterwards, linear elastic FEM (Finite Element Method) and DBEM (Dual Boundary Element Method) [12-19] bidimensional stress analyses were performed to simulate crack growth.

Numerical and experimental results exhibit a satisfactory degree of correlation.

2. Experimental test

In this study experimental crack growth tests on Friction Stir Welding (FSW) welded flat stiffened panels have been performed. The stiffened panel shown in Fig. 1.a is composed of two "Z" shape stringers (1.3 mm thick), joined to a flat panel, 300x500x1.3 mm^3 sized, by two double continuous lap-welding joint. Run-in and run-out of welding lines have been cut before starting the test so that the final sizes of the panel turn out to be 300x370 mm^2.

A central notch has been created to predefine the crack initiation site: its length is equal to 14 mm and is cut by Electrical Discharge Machining (EDM) (Figs. 1.b-c); the notch direction (horizontal) is perpendicular to the load direction.

Panels and stiffeners are made of aluminium alloy 2024 T3 whose mechanical properties are given in Table 1.

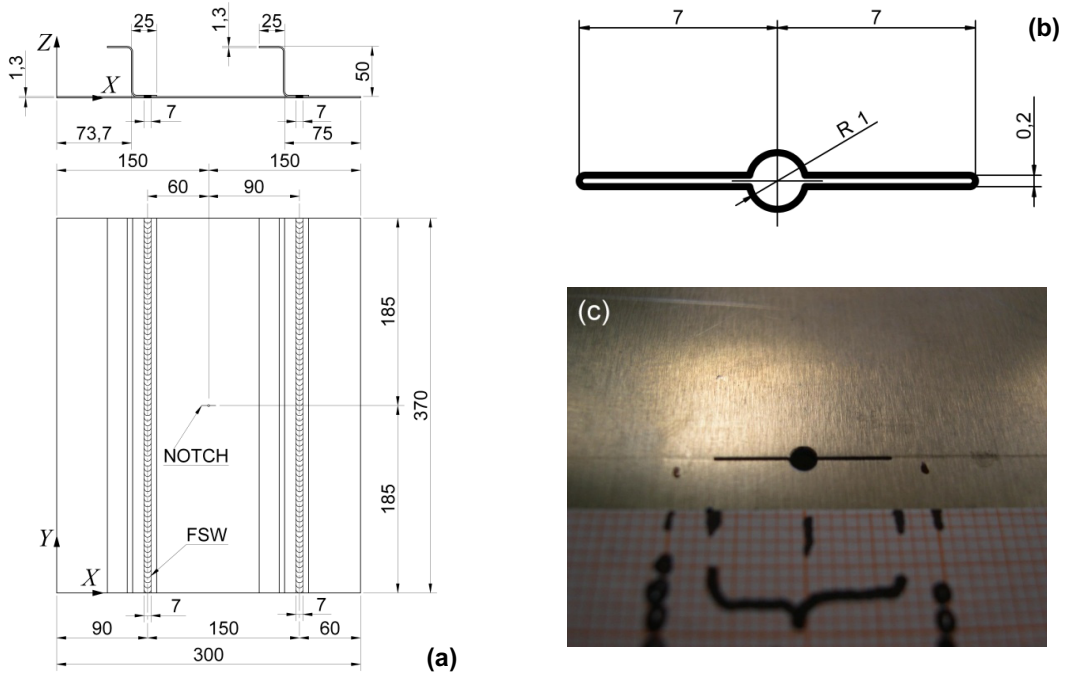

Fig. 1. (a) Specimen geometry; (b) notch sizes; (c) detail of the notch made by EDM (the crack is also visible).

Scope of the performed tests was to evaluate fracture arrest capability of the FSWelded stiffeners applied on the flat panel when an artificial crack is introduced and propagated due to fatigue loads.

Table 1. Mechanical properties of 2024-T3.

Property	Value
Young's modulus	70000 [MPa]
Tensile Strength	448 [MPa]
Yield Strength	331 [MPa]
Crack growth threshold	100.77 [MPa·mm$^{1/2}$]
Poisson ratio	0.33

The testing machine (Fig. 2.a) is composed by a hydraulic actuator (max load P_{max} = 60 kN) connected to an external rigid frame, with a load cell (100 kN max range). The load is applied along the whole width of the panel by means of bolted grips interposed between actuator and panel (Fig. 2.b). The grip fixture has been designed in order to enforce a load introduction exactly in the skin middle plane avoiding any rotation or eccentricity. In fact, in order to reduce the eccentricity, a special plate has been bonded on both sides of the stiffened panel by using a bi-component methacrylate structural adhesive MA 420 of Plexus (ultimate strength 18.6 MPa). Bonded strips for both sides are 20 mm wide to assure a uniform load distribution on all test coupons.

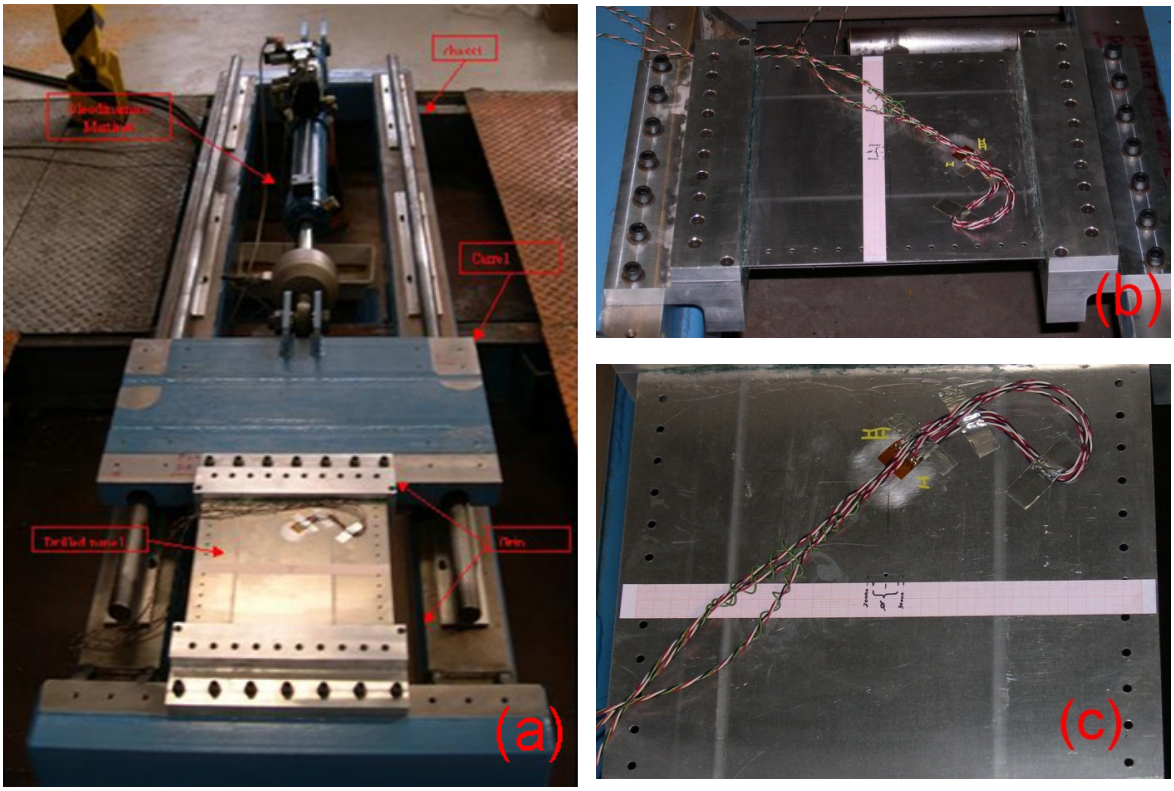

Fig. 2. (a) Testing machine; (b) bolted grips; (c) test panel with highlight of strain rosette.

A strain rosette (Fig. 2.c), type CEA-13-250UR-350 of MM Vishay, was bonded on each panel side, in order to verify the absence of secondary bending and assess the consistency of measured local stress against those forecasted in the design phase. The fatigue tests were carried out under constant amplitude load control (R = 0.1, P_{max} = 43.65 kN) with frequency equal to 5 Hz and a preliminary load was applied to reduce internal clearance of grip fixture. All tests were performed at room temperature.

During the test, crack propagation has been monitored from its start at the two tips of the notch up to the progressive skin and/or stringer failure. In the first part of the propagation, the crack length was observed using a 4X optical magnifier and the crack tip advance measured with a micrometer. When the crack advance reached the size of 20 mm, an inspection plan was set up at intervals of 10000 cycles; the esteem of crack propagation extension took advantage of graph paper bonded on panels (Fig. 1.c).

3. Numerical model

FEM and DBEM models have been developed with the aim of investigating the crack parameters during crack propagation . A model of the whole panel has been developed and crack propagation is simulated by using both a commercially available finite element code (ANSYS) and boundary element code (BEASY). The material behavior has been modeled as linear elastic.

3.1. FEM model

The panel was modeled using two-dimensional eight-node shell elements (SHELL 93), with each node having six degrees of freedom, and two-dimensional eight-nodes plane elements (PLANE 82), with each node having two degrees of freedom. The finite element mesh (Fig. 3.a) consists of 1708 elements and 4989 nodes (different colors are associated to different type of elements). Shell and plane elements were used to model stringers and skin respectively.

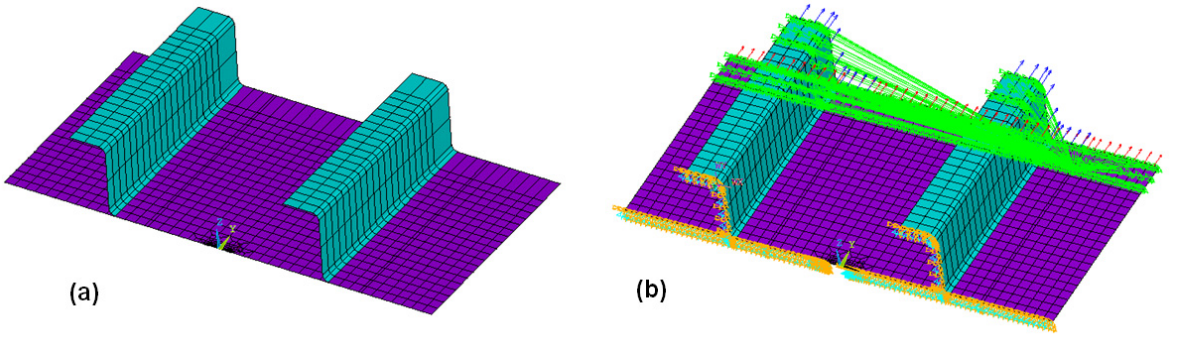

Fig. 3. (a) 3D FE model of the panel; (b) boundary conditions applied to the panel.

FEM crack analysis takes advantage of special quarter-point elements (the mid-point nodes are shifted to the quarter-point locations to account for the crack tip singularity) and SIFs are calculated by the crack opening displacement method (COD). The welding between skin and stringers was modeled by merging the nodes of skin and stringers along the welding line. It is possible to benefit of a plane of symmetry XZ for the problem, therefore only half panel was modeled.

At one model end the symmetry constrains were applied whereas on the other end a nominal pressure p = 69.5 MPa (P = 43.65 kN) was applied in Y direction; moreover, to simulate the grip fixture, rigid constrains were applied along a strip 20 mm wide. In Fig. 3.b the boundary conditions applied to the panel are shown.

3.2. DBEM model

The two-dimensional DBEM model, realized by the commercial software BEASY [20], is shown in Fig. 4.a with highlight of each single component (panel, stiffeners, grip fixture, notch). The model is divided in four zones (Fig. 4.b): the skin is modeled as zone 1 with a thickness equal to 1.3 mm and related material properties as reported in Table 1; the grip plate is modelled as zone 3; the two stringers are modeled as zone 2 and 4. The latter are to be split in two different zones in order to allow the crack to propagate in the skin without "affecting" the approaching stiffener that fails only after that the crack has overcome it (the modeling procedure is detailed in [16]). In particular, two layers, overlapped in correspondence of the stiffener area, are modeled, the first representative of the skin and affected by the crack propagation and the second to model the stiffener.

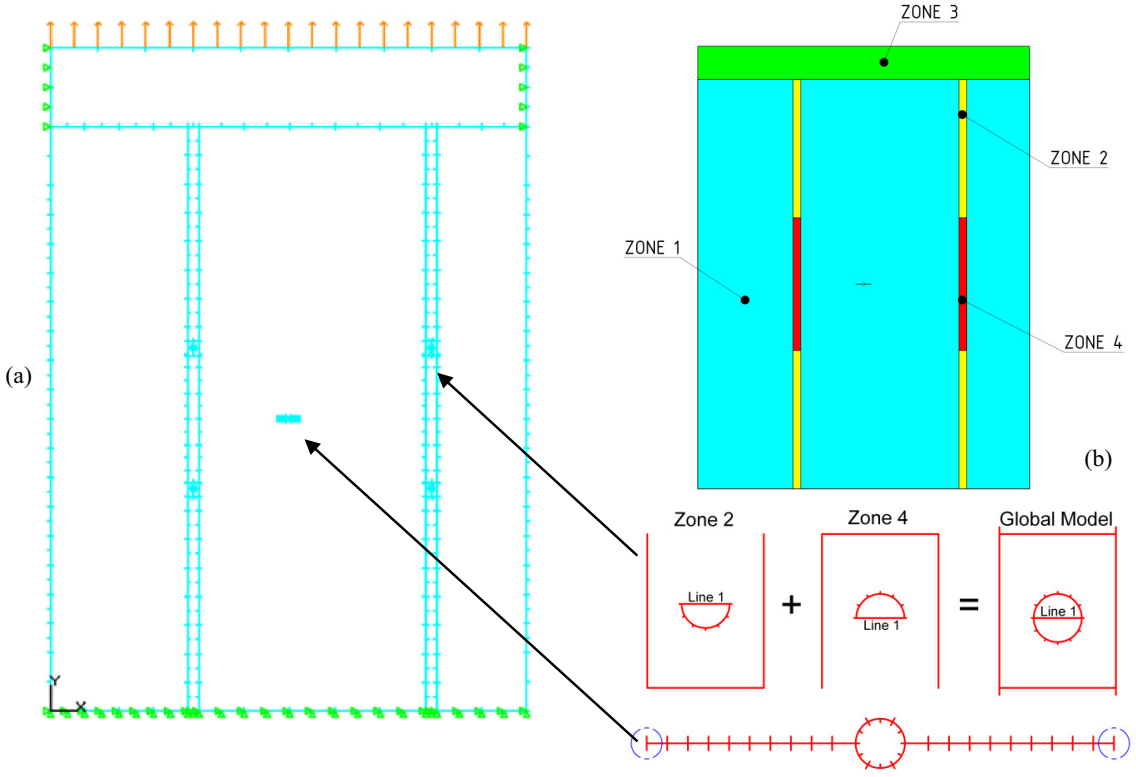

Fig. 4. (a) 2D DBEM model of the panel with close up of initial crack and interface line 1 to connect zone 2 and zone 4; (b) highlight of zones with different thickness.

The stiffeners are modeled with a width equal to 7 mm, corresponding to the width of the welding line. The thickness of zone 2 is equal to 18.65 mm: such value makes the transversal area equal to the transversal area of the real stiffener plus the corresponding transversal area of the overlapped skin part. Zone 4 has a thickness equal to 17.35 mm that is the thickness of zone 2 minus skin thickness, since this zone is representative of a layer overlapped but distinct from the skin layer. The material properties of zones 2 and 4 are the same as those of zone 1. The connection between zones 2 and 4 is modeled by half circles (Fig. 4.a): this is just an artifice to provide continuity between the two parts in which the stringer is subdivided [16]. With this type of modeling the 2D DBEM model can reproduce the same membrane stiffness of the tested panel. The fixture on which the load is applied is modeled by zone 3. The thickness of this zone is equal to 30 mm, the Young modulus 200000 MPa and the Poisson ratio 0.3: with such a high thickness value zone 3 nearly performs as a rigid body, constraining the panel to have a uniform Y displacement along the upper side.

As shown in Fig. 4.a, the lower side of the panel is constrained in both X and Y directions whereas constraints in X direction are applied on the left and right side of the grip fixture. Tractions are applied along Y direction in such a way to provide a resultant load P = 43.65 kN as used in the experimental test. Two cracks initiated from hole sides are introduced to model notch (Fig. 4.a). The overall mesh is based on nearly 150 quadratic elements (with more than 800 dofs); such number will slightly increase during crack propagation. Discontinuous quadratic elements are used to model the crack.

4. Results and discussion

Figs. 5.a-b show the direct stresses σ_{yy} [MPa] in correspondence of the initial crack scenario (the initial notch is approximated by a crack) evaluated by FEM and DBEM analyses respectively.

The first monitored experimental cracked scenario is based on two cracks from the two sides of the notch (Fig. 1.c) with a length equal to 0.5 mm on each side.

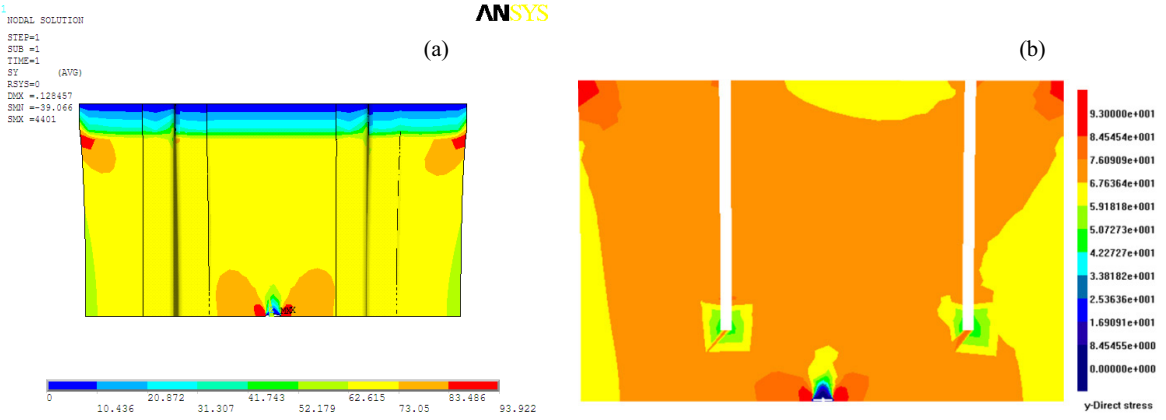

Fig. 5. Direct stresses σ_{yy} [MPa] evaluated by FEM (a) and DBEM (b).

In DBEM simulation, SIF evaluation is based on the J-integral method [12]: a set of internal points, along a circular path (with symmetrical positions with respect to the crack axis) defines the contour along which the J-integral is calculated (Fig. 4.a).

Fig. 6 shows the stress scenario evaluated by FEM and DBEM models after 148741 cycles of crack propagation ($2a$ = 42 mm): the DBEM color map appears rough because of a limited number of internal points available for triangulation.

The crack growth law adopted for the propagation in the aluminum layer is the NASGRO 4.0 equation (Eq. 1):

$$\frac{da}{dN} = C\left[\left(\frac{1-f}{1-R}\right)\Delta K\right]^n \frac{\left(1-\frac{\Delta K_{th}}{\Delta K}\right)^p}{\left(1-\frac{K_{\max}}{K_{crit}}\right)^q} \tag{1}$$

whose calibration parameters are those related to AL 2024-T3 (Table 2).

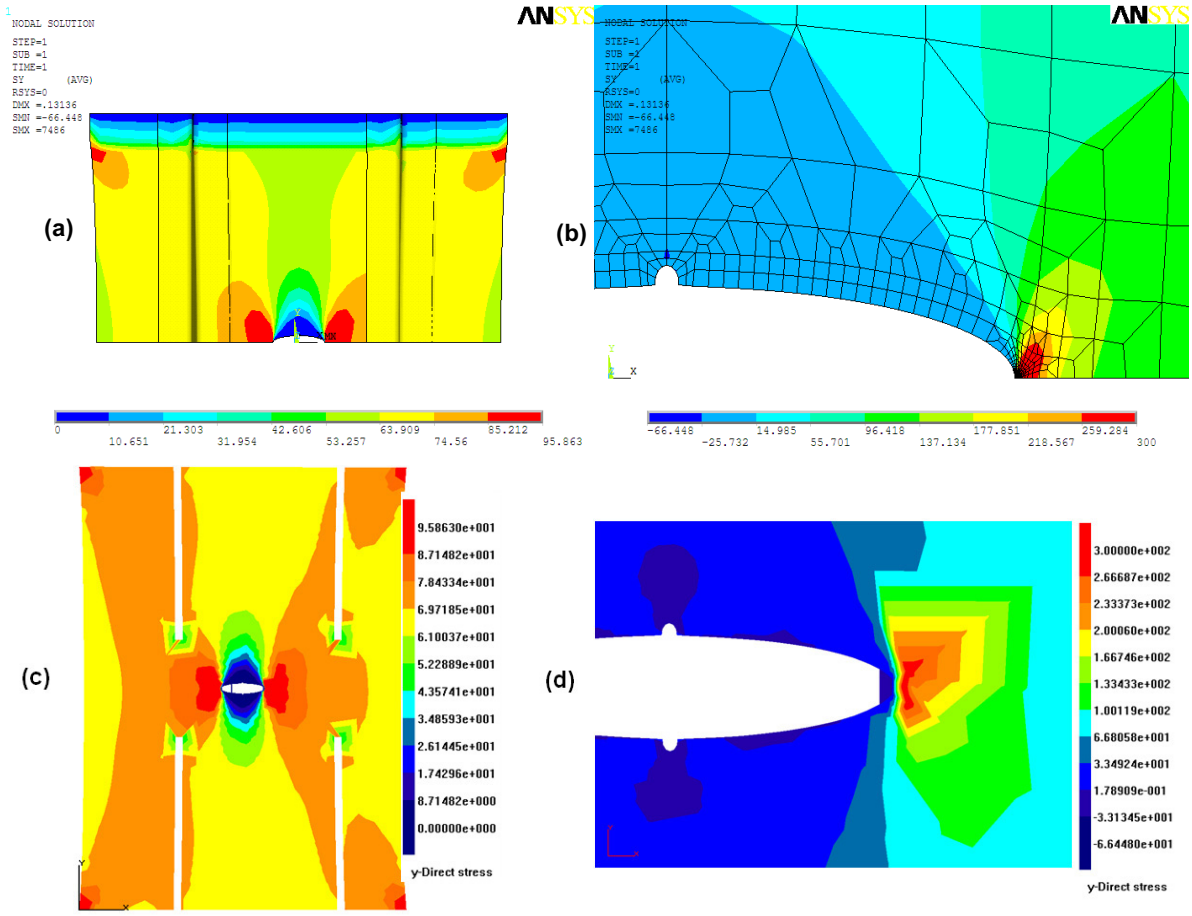

Fig. 6. Direct stresses σ_{yy} [MPa] evaluated by FEM and DBEM (a, c- overall views, b, d - detail views nearby crack tip).

Table 2. Fitting parameters for the AL 2024-T3 from NASGRO library (SIF in [$MPa*mm^{0.5}$] and length in [mm]).

Parameter	Value
Part through fracture toughness (K1E)	1425
Plane strain fracture toughness (K1C)	1008
AK Coefficient (AK)	1.0
BK Coefficient (BK)	1.0
Crack growth rate coefficient (C)	2.44 ·E-11
N Coefficient (N)	2.601
P Coefficient (P)	0.5
Q Coefficient (Q)	1
Threshold SIF at R=1 (DK1)	101
C Threshold positive value (CPTH)	1.5
Plane stress strain constraint factor (ALFA)	1.5
S.R. Ratio (SR)	0.3
Intrinsic crack length (A0)	0.0381

From FE and DBEM analyses, it comes out that the two crack tips proceeds with nearly the same growth rate, but, due to the different initial distance from the stiffeners, the left tip reaches the stiffener before than the right tip (Fig. 7.a). At this stage the two stiffeners are still both intact providing a relevant “bridge effect” as visible from the stress scenario in Fig. 7.b.

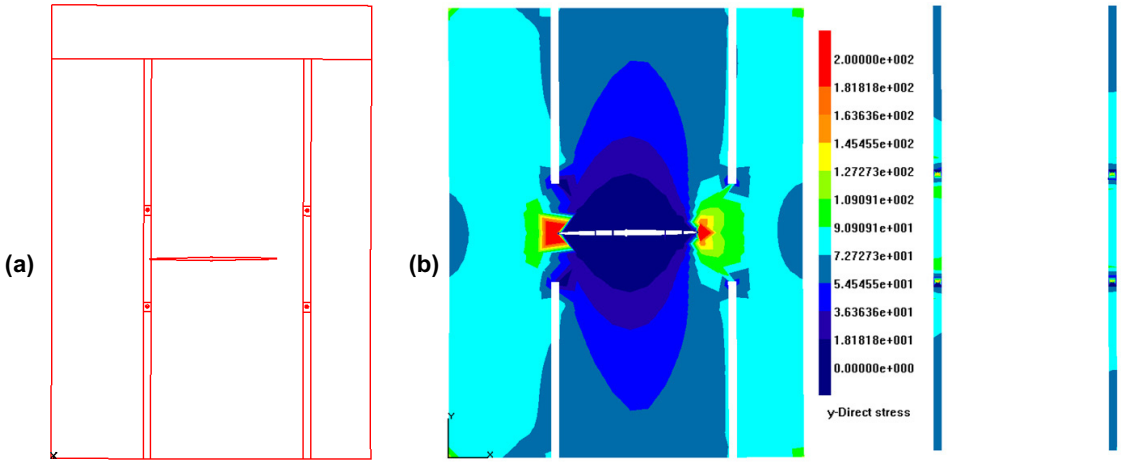

Fig. 7. (a) deformed plot; (b) direct stress σ_{yy} [MPa] scenario when the left tip reaches the stiffener.

The crack propagation under the stiffeners was not simulated by FEM but this limitation was circumvented by the DBEM approach. In fact, when the crack length on the left side reaches a length equal to 62 mm (Fig. 8) the approached left stiffener breaks down (no load transfer anymore), and so the stiffness of the whole panel suddenly decreases with consequent sharp acceleration in the crack propagation on both sides (Fig. 9). Such scenario can be simply reproduced by the DBEM model in the following way: when the left side of the crack reaches the length of 62 mm (Fig. 8), in order to simulate the left stiffener failure, zone 2 and left part of zone 4 can be simply disconnected by introducing internal springs of negligible stiffness on the interface connection line 1 (Fig. 4.a). From this point on there is no load transfer anymore from the left stiffener that becomes unloaded in its central part as visible from Fig. 8.b.

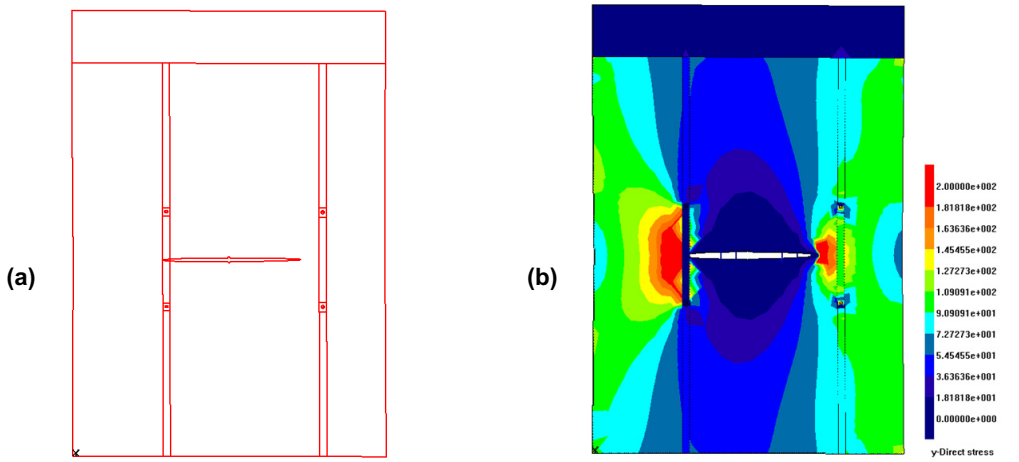

Fig. 8. (a) DBEM deformed plot of the panel when $2a$ = 62 mm; (b) DBEM direct stress σ_{yy} [MPa] in Y direction.

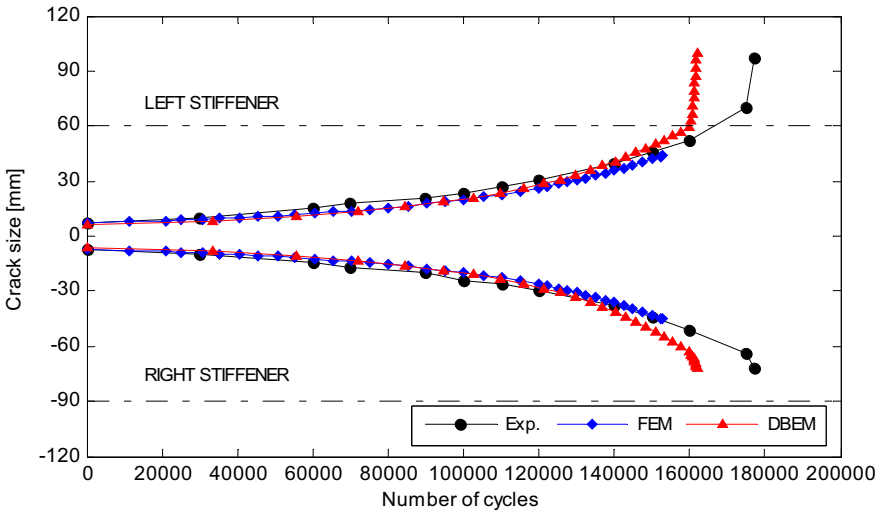

Fig. 9. Crack size [mm] vs. number of cycles for the two cracks.

The experimental propagation recording proceeds up to a number of cycles equal to 177000: at this stage the panel breaks down (Fig. 10). As Fig. 10 shows, the extension of plastic zone surrounding the crack tip is still not affecting the main part of the residual ligament so that a panel failure for plastic collapse can be excluded; consequently the panels fails due to fracture instability. This is confirmed by the K_I values in the final stage of crack propagation (Fig. 11) getting close to the (plane stress) fracture toughness (nearly 2000 MPa·mm$^{0.5}$) calculated for the material under analysis and in correspondence of the related skin thickness (Eq. 2).

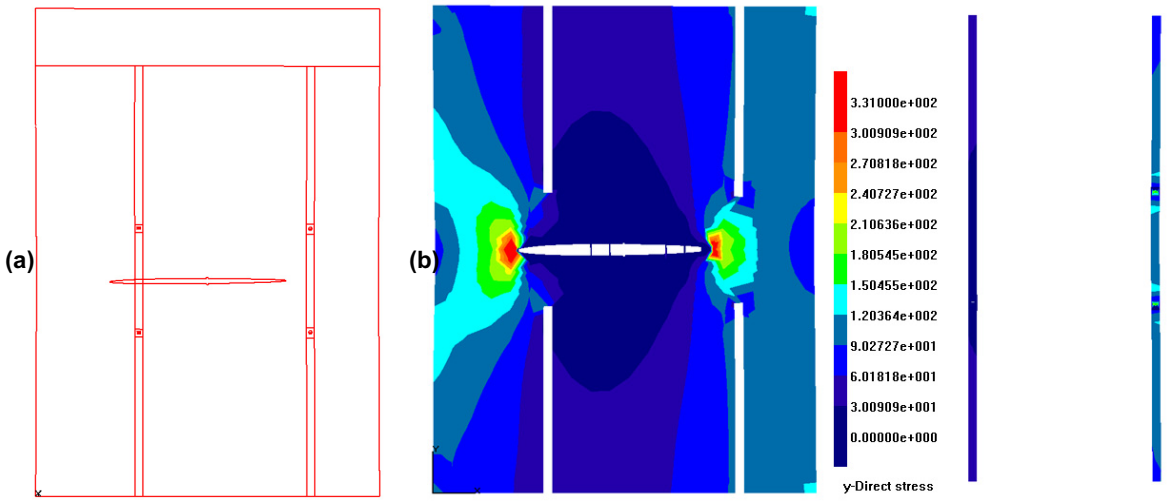

Fig. 10. (a) deformed scale; (b) direct stress scenario σ_{yy} [MPa] after fatigue test.

FEM and DBEM Stress Intensity Factors (SIF's), calculated in correspondence of different crack sizes, are shown in Fig. 11 and turn out to be in a satisfactory agreement.

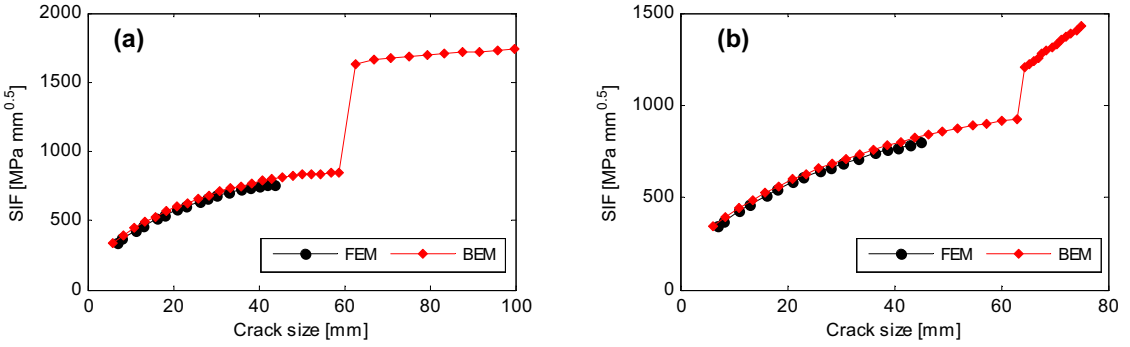

Fig. 11. SIF's vs. crack size for the two cracks: (a) left side; (b) right side.

$$\frac{K_C}{K_{IC}} = 1 + BK \cdot e^{-\left(AK \cdot \frac{t}{2.5\left(\frac{K_{IC}}{\sigma_y}\right)^2} \right)^2} \tag{2}$$

In Fig. 12 the broken panel after the fatigue test is shown: it is possible to observe that one stiffener remains intact even after the panel failure and this is confirmed also by the DBEM analysis (Fig. 10.b), showing a level of stress in the intact stiffener still below the yielding values.

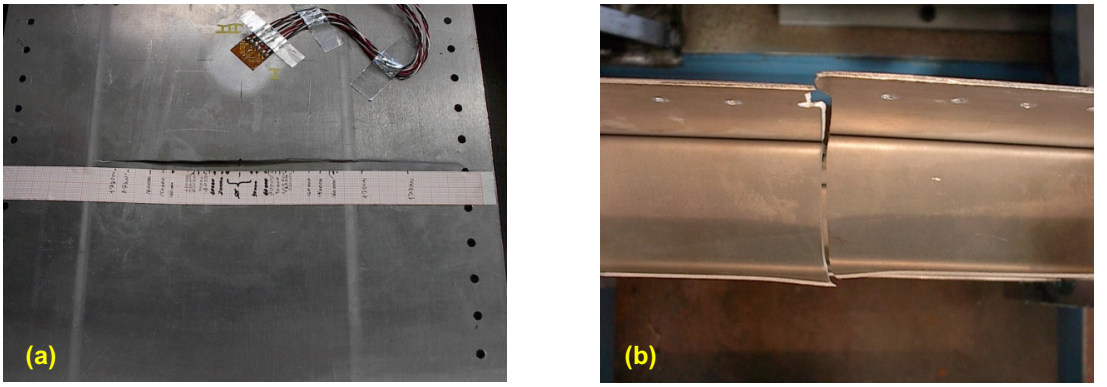

Fig. 12. (a) final failure of the panel at 177000 cycles; (b) detail of stringer failure.

5. Conclusion

In this study experimental tests and numerical approaches have been used to evaluate fracture arrest capability of FSWelded stiffeners on flat panel with the presence of an artificial crack, subjected to fatigue loads. FE model and DBEM model of the whole panel specimen have been developed to investigate the crack propagation. The correlation between numerical and experimental results is judged satisfactory. The DBEM procedure can more efficiently and accurately take the complicate stress scenarios arising when the crack approaches the stiffener.

References

[1] R.J.H. Wanhill, L. Molent, S.A. Barter, Fracture mechanics in aircraft failure analysis: Uses and limitations, Eng. Fail. Anal. 35 (2013) 33–45.

[2] F Caputo, G Lamanna, A Soprano, Numerical investigation on the crack propagation in a flat stiffened panel, Key. Eng. Mat. 324-325 (2006) 1039-1042.

[3] J. Schijve, The significance of fatigue crack initiation for predictions of the fatigue limit of specimens and structures, Int. J. Fatigue. 61 (2014) 39-45.

[4] F Caputo, G Lamanna, A Soprano, Residual strength improvement of an aluminium alloy cracked panel, The Open Mechanical Engineering Journal. 7 (2013) 90-97.

[5] G Lamanna, F Caputo, A Soprano, Stochastic improvement of the residual strength of a stiffened panel, Key. Eng. Mat. 348-349 (2007) 301-304.

[6] L. Molent, S.A. Barter, A comparison of crack growth behaviour in several full-scale airframe fatigue tests, Int. J. Fatigue. 29 (2007) 1090-1099.

[7] S.S. Wang, R.C. Chu, Full scale fatigue crack growth test of advanced jet trainer AT-3, Theor. Appl. Fract. Mec. 11 (2) (1989) 71-91.

[8] R. Sepe, E. Armentani, F. Caputo, G. Lamanna, Fatigue behaviour of full scale flat stiffened aeronautic panels, Key. Eng. Mat. 627 (2015) 97-100.

[9] M. Giglio, A. Manes, Crack propagation on helicopter panel: Experimental test and analysis, Eng. Fracture Mechanics. 75 (2008) 866–879.

[10] E. Armentani, R. Citarella, R. Sepe, FML Full Scale Aeronautic Panel Under Multiaxial Fatigue: Experimental Test and DBEM Simulation, Eng. Fract. Mech. 78 (8) (2011) 1717-1728.

[11] E. Armentani, F. Caputo, R. Esposito, G. Godono, A New Three Loading Axes Machine for Static and Fatigue tests, Proceedings of the Sixth International Conference on Biaxial/Multiaxial Fatigue & Fracture, Lisboa, Portugal, 1 (2001) 323-330.

[12] Rigby RH, Aliabadi MH. Mixed-mode J-integral method for analysis of 3D fracture problems using BEM, Eng. Anal. Boundary Elem. 11 (1993) 239–56.

[13] C. Calì, R. Citarella, M. Perrella, Three-dimensional crack growth: numerical evaluations and experimental tests, European Structural Integrity Society, Biaxial/Multiaxial Fatigue and Fracture, Edited by Andrea Carpinteri, Manuel de Freitas and Andrea Spagnoli, 31 (2003) 3-504

[14] C. Calì, R. Citarella, Residual strength assessment for a butt joint in MSD condition, Adv. Eng. Softw. 35 (2004) 373-382.

[15] R. Citarella, M. Perrella, Multiple surface crack propagation: numerical simulations and experimental tests, Fatigue Fract. Eng. M. 28 (2005) 135-148.

[16] E. Armentani, R. Citarella, DBEM and FEM analysis on non-linear multiple crack propagation in an aeronautic doubler-skin assembly, Int. J. Fatigue. 28 (2006) 598–608.

[17] R. Citarella, Non Linear MSD crack growth by DBEM for a riveted aeronautic reinforcement, Adv. Eng. Softw. 40 (4) (2009) 253–259.

[18] R. Citarella, MSD Crack propagation on a repaired aeronautic panel by DBEM, Adv. Eng. Softw. 42 (10) (2011) 887-901.

[19] R. Citarella, G. Cricrì, E. Armentani, Multiple crack propagation with Dual Boundary Element Method in stiffened and reinforced full scale aeronautic panels, Key. Eng. Mat. 560 (2013) 129-155.

[20] BEASY V10r14. Documentation. C.M. BEASY Ltd. (2011).